Journal of Neuroinflammation

RESEARCH

Open Access

Cholecystokinin ameliorates cognitive impairment via inhibiting microglia phagocytosis of excitatory synapses in sepsis-associated encephalopathy mice

Lei Chen[1], Zhen Li[2], Yubo Gao[3], Guangxi Piao[4], Yitong Li[1], Jingshu Hong[1], Qian Wang[1], Kaixi Liu[1], Jie Wang[5,6], Ailian Du[5], Luhua Chen[7,8,9], Xiangyang Guo[1], Zhengqian Li[1,10,11*] and Taotao Liu[1*]

Abstract

Background Sepsis-associated encephalopathy (SAE) is characterised by cognitive impairment and is a common complication in patients with sepsis. Microglia are involved in various cognitive impairment-related diseases through phagocytic synapses. Cholecystokinin (CCK), an abundant neuropeptide in the brain, is closely related to cognitive function. However, the role of CCK in SAE and the relationship between CCK and microglial phagocytosis of synapses are unknown.

Methods Lipopolysaccharide (LPS) was used to construct SAE models in 3-month-old male mice and BV2 microglial cells. To investigate the effects of CCK on cognitive impairment in SAE model mice, we used exogenous CCK injection into the dorsal hippocampal CA1 region or the chemogenetic activation of CCK-positive neurons to promote endogenous CCK release. Morris water maze and fear conditioning test were used to assess cognitive function in mice. RNA sequencing was performed to explore the potential signalling pathways involved in CCK-induced neuroprotection. Western blot and immunofluorescence were used to assess the effects of CCK on microglial phagocytosis of synapses, neurotoxic astrocytes, and excitatory synapses. Whole-cell recording was used to determine excitatory synaptic transmission.

Results LPS successfully established in vivo and in vitro models of SAE. Both exogenous CCK injection and activation of CCK-positive neurons in hippocampal CA1 region attenuated cognitive impairment in SAE mice. Mechanistically, CCK significantly alleviated excitatory synaptic plasticity damage via inhibiting complement 1q (C1q)-mediated microglial phagocytosis of synapses and neurotoxic astrocyte polarisation. Moreover, in vitro SAE model of BV2 cells demonstrated that CCK exerts neuroprotective effects through microglial CCK2-type receptor.

*Correspondence:
Zhengqian Li
zhengqianli@hsc.pku.edu.cn
Taotao Liu
liutaotao1101@163.com

Full list of author information is available at the end of the article

Conclusions CCK may alleviate cognitive impairment by inhibiting microglia C1q-mediated phagocytosis of excitatory synapses, suggesting that both CCK drugs and specific activation of CCK-positive neurons are potential treatments for SAE.

Keywords Sepsis-associated encephalopathy, Cholecystokinin, Microglia, Complement 1q, Excitatory synapse

Introduction

Sepsis-associated encephalopathy (SAE) refers to sepsis-induced diffuse or multifocal brain dysfunction, excluding that caused by direct brain infection and other diseases [1]. SAE is the most common encephalopathy in the intensive care unit [2], with a prevalence of up to 70% in patients with sepsis and an annual incidence of approximately 750,000 cases in the United States alone [3]. Compared with patients without neurological symptoms, patients with SAE have significantly extended hospitalisation periods and a 26–49% increase in mortality, which brings serious harm to society and families [4]. Although there are many hypotheses regarding the pathogenesis of SAE, including blood–brain barrier damage, oxidative stress, brain microenvironment dysfunction, and the abnormal activation of glial cells, there remains a lack of effective treatments [5]. It is therefore crucial to explore the pathogenesis of SAE and develop effective therapeutic measures.

Neuropeptides are widely distributed in the central nervous system (CNS); they act as neurotransmitters or neuromodulators to mediate communication between neurons and other cells [6]. Cholecystokinin (CCK) was one of the first neuropeptides to be identified, and is widely distributed in brain regions such as the hippocampus and amygdala, as well as in the peripheral digestive system. CCK can be sheared to form many isoforms of different lengths; CCK8 is one of the most abundant isoforms and has all of the biological functions of CCK [7]. Our previous study demonstrated that intraperitoneal CCK8 injection improves postoperative delayed neurocognitive recovery in aged mice [8]. Another study demonstrated that CCK8 enhances spatial memory performance in the Morris water maze (MWM) in wild-type rodents [9], and electrophysiological recordings indicate that CCK8 can induce long-term potentiation in the cornu ammonis 1 (CA1) subregion of rat hippocampal slices [10]. However, it remains unclear whether CCK8 ameliorates synaptic plasticity and cognitive impairment in SAE model mice.

Microglia are the resident immune cells in the CNS, and previous studies have mainly focused on their role in modulating the inflammatory response [11]. In recent years, microglia have also been demonstrated to play an important role in pruning excessive synapses in the developing brain, as well as in synaptic dynamics in the adult brain [12]. The role of microglia in regulating synaptic function has therefore attracted the attention of researchers. Microglia-mediated synaptic pruning involves the classical complement pathway (part of the innate immune system), which contributes to the phagocytic removal of microbes and damaged cells [13]. In particular, C1qa microglial-produced protein and the promoter of the classical complement system in the brain-localises at synapses and mediates synaptic elimination via phagocytic microglia [14]. In addition, C1q can cause an increase in neurotoxic reactive astrocytes (also termed A1 astrocytes), thereby damaging synapses [15]. Gou et al. reported that CCK8 is anti-inflammatory via its inhibition of microglial activation, similar to the findings of our previous study [8, 16]. However, it remains unclear whether CCK attenuates cognitive impairments by inhibiting microglial C1q-dependent synaptic loss in SAE model mice.

In the present study, we therefore aimed to assess the role of CCK and CCK-positive neurons of the dorsal hippocampus CA1 region in improving cognitive function in SAE mice. We hypothesised that CCK attenuating C1q-mediated synaptic plasticity damage and ultimately improving cognitive dysfunction in SAE mice.

Methods

Animals

Wild-type C57BL/6 mice were purchased from the Peking University Health Science Center Department of Laboratory Animal Science (Beijing, China), and CCK-Cre (C57 background) mice were gifted by the laboratory of Professor Miao He (Institutes of Brain Science, Fudan University). The mice were housed eight per cage on a 12-h light/dark cycle in a temperature-controlled room (20 °C ± 2 °C) with free access to water and food. The mice were acclimatised to the environment for 7 days before the experiments, and 3-month-old male mice were used for all experiments. The protocol was approved by the animal ethics committee of Peking University Health Science Center (ethics number: LA2021534). All experiments followed the Guiding Principles for the Care and Use of Animals in Research and the Animal Research: Reporting of In Vivo Experiments (ARRIVE) 2.0 guidelines [17].

SAE mouse model

In accordance with previous studies [4, 18], a single intraperitoneal injection of 5 mg/kg LPS from *Escherichia coli* O55:B5 (Sigma-Aldrich, St. Louis, MO, USA, Cat. No. L2880) was dissolved and diluted in endotoxin-free

phosphate-buffered saline to establish the SAE mouse model. For 7 days after the LPS injection, the body weight and sepsis score of each mouse was recorded daily [19]. The sepsis score was based on the consciousness level, spontaneous activity, response to touch and auditory stimuli, respiration rate and quality, and appearance. Each of these variables was given a score from zero to four by trained research staff; higher scores indicated more severe symptoms of sepsis. Mice were euthanised if the sepsis score was >21 or if the respiratory quality or rate increased by more than three at any time. Of the 13 mice injected with LPS, only one died on the second day after injection, which is similar to the survival rate reported in previous study [20].

Cannula implantation and viral injection

Mice were fixed on the stereotaxic apparatus under 1–2% sevoflurane anaesthesia. For pharmacological experiments, a bilateral cannula (RWD Life Science, Shenzhen, China) was implanted into the dorsal hippocampal CA1 (anteroposterior: −2.00; mediolateral: ±1.50; dorsoventral: −1.35; mm relative to bregma) for the infusion of CCK8 or L365,260 (a CCK2 antagonist). The coordinates were selected using the Mouse Brain in Stereotaxic Coordinates (Third Edition). One stainless steel screw was implanted in the skull for reinforcement, and the cannula and screw were secured using dental cement.

For the chemogenetic experiments, we performed a bilateral stereotaxic injection of 100 nL AAV2/9-Ef1α-DIO-hM3Dq-mCherry-WPREs (activation virus) or AAV2/9-Ef1α-DIO-mCherry-WPREs (control virus) (BrianVTA, Wuhan, China, Cat. No. PT-0042) into the hippocampal CA1 (anteroposterior: −2.00; mediolateral: ±1.50; dorsoventral: −1.40; mm relative to bregma) at a rate of 30 nL/min. The needle was left in place for 10 min after the infusion before being slowly withdrawn. Two weeks later, the mice were used for experiments. Thirty minutes before behavioural testing, an intraperitoneal injection of 5 mg/kg clozapine N-oxide was used to activate the CCK-positive neurons.

MWM

The MWM is commonly used to assess hippocampus-dependent learning and memory in mice [8]. The MWM equipment (Sunny Instruments Co. Ltd., Beijing, China) consisted of a cylinder (diameter: 120 cm, height: 50 cm) with a video camera positioned above it. The MWM was divided into four quadrants, and the quadrant containing the platform was termed the target quadrant. Milk powder was added to the water to easily distinguish each mouse from the background, and the water temperature was maintained at 21 °C ± 1 °C.

The MWM test comprised a place navigation test and a spatial probe test. In the place navigation test, the mice were gently placed into quadrants facing the wall of the maze, and were then allowed to search for the platform (placed 1 cm underwater) for 60 s. The taken time to locate the platform was recorded and defined as the escape latency. If the mouse was unable to find the platform within 60 s, it was guided to the platform and left there for 15 s, and the escape latency was recorded as 60 s. In the spatial probe test, the submerged platform was removed, and the latency to the platform, number of platform crossings, and time spent in the target quadrant of mice were recorded over a 60 s period. Swimming speed was recorded throughout the tests to rule out any influence of changes in exercise capacity on the experimental results.

Fear conditioning test (FCT)

The FCT detects changes in fear memory in mice, and includes training and testing phases [21]. The training phase was performed 1 day before LPS injection. Mice were Gently placed into the FCT chamber for 3 min, followed by 20 s of sound stimulus (80 dB, 5000 Hz) and 1 s of electrical foot-shock (0.8 mA) after a 20-s interval for two cycles. This phase was used to build up fear memory related to the experimental background, acoustic sound, and electrical foot-shock.

The testing phase consisted of context and tone tests on day 3 after LPS injection. The context test was performed first. In this test, the mice were placed in the same background as the training phase of the chamber and allowed to explore freely for 5 min. The freezing time of the mice was recorded, reflecting hippocampus-dependent fear memory. The tone test was performed 2 h after the context test. In this test, the background pattern of the chamber was changed to exclude the interference of context memory. The mice were placed in the chamber for 3 min and then given a sound stimulus (80 dB, 5000 Hz) for 20 s for two cycles, and the freezing time was recorded; this mainly reflected non-hippocampus-dependent fear memory [11]. Tracking system software (Macroambition S&T Development Co. Ltd., Beijing, China) was used to record the total distance travelled and the freezing time. After each test session, the chamber was wiped with 75% alcohol to avoid any effects of odour.

BV2 cell culture and treatment

The immortalised murine BV2 microglial cell line was purchased from China Infrastructure of Cell Line Resource (Beijing, China). Cells were cultured in Dulbecco's modified Eagle medium (Thermo Fisher Scientific, Waltham, MA, USA, Cat. No. C11995500BT) containing 10% foetal bovine serum (Gibco, Invitrogen, Grand Island, NY, USA, Cat. No. 10270106) and 1% penicillin/streptomycin at 37 °C under 5% CO_2 and 95% air.

Stimulation of BV2 cells by LPS was used to establish a microglial in vitro model of SAE. On the basis of previous studies [22, 23], we chose different concentrations of LPS (0.1, 0.2, 0.5, 1, and 2 μg/mL) to stimulate BV2 cells for various amounts of time (1, 3, 6, 12, and 24 h). To determine the most suitable LPS concentration and duration for the present study, C1q expression was evaluated.

Next, to select the effective dose of CCK8 for inhibiting C1q expression, different doses of CCK8 (0.2, 0.5, 1, and 2 μM, Tocris, Bristol, UK, Cat. No. 1166) were used. After determining the effective dose of CCK8, we used the CCK2R antagonist L365,260 (10 μM, Tocris, Cat. No. 2767) and the CCK1R antagonist SR27897 (10 μM, Tocris, Cat. No. 2190), based on previous literature, to validate the receptors responsible for CCK8 action [16].

The culture medium from BV2 cells was placed in a centrifuge tube and centrifuged to remove detached cells and cell debris. Subsequently, the Liquid Sample Protein Recovery Kit (Applygen, Cat. No. P1255) was used to extract proteins from the culture medium for the detection of extracellular proteins. After washing the BV2 cells in the culture dish twice with pre-cooled PBS, the BV2 cells were transferred to a centrifuge tube for the intracellular protein detection.

Western blotting

Mice were euthanised by cervical dislocation, and the bilateral hippocampus was isolated on ice. Hippocampal tissues or BV2 cells were then placed in radioimmunoprecipitation lysis buffer containing protease (Applygen, Cat. No. P1265) and phosphatase (Applygen, Cat. No. P1260) inhibitors and subsequently homogenised using a grinder (Verder Shanghai Instruments and Equipment Co., Ltd., Shanghai, China). The lysate was centrifuged at 12,000 × *g* (15 min, 4℃) and the supernatant was collected. A bicinchoninic acid protein assay kit (Applygen, Cat. No. P1511) was used to detect the protein concentration. Next, protein samples were separated by 10% sodium dodecyl-sulphate polyacrylamide gel electrophoresis and transferred to polyvinylidene difluoride membranes (Millipore, Billerica, MA, USA, Cat. No. IPVH00010). The membranes were blocked with 5% Albumin Bovine V (Solarbio, Beijing, China, Cat. No. A8020) in Tris-buffered saline containing 0.1% Tween 20 (TBST) for 1 h at room temperature. They were then incubated overnight at 4℃ with the following primary antibodies: rabbit anti-CCK-8 (1:1000, Immunostar, Hudson, WI, USA, Cat. No. 20078, RRID: AB_572224), rabbit anti-C3 (1:1000, Proteintech, Wuhan, China, Cat. No. 21337-1-AP, RRID: AB_2878843), mouse anti-glial fibrillary acidic protein (GFAP; 1:1000, Boster, Wuhan, China, Cat. No. BM0055, RRID not available), mouse anti-postsynaptic density protein 95 (PSD95; 1:1000, Cell Signaling Technology, Danvers, MA, USA, Cat. No. 36233, RRID: AB_2721262), rabbit anti-vesicular glutamate transporter 1 (vGlut1; 1:1000, Abcam, Cambridge, UK, Cat. No. ab227805, RRID: AB_2868428), rabbit anti-C1q (1:1000, Abcam, Cat. No. ab182451, RRID: AB_2732849), and rabbit anti-β-actin (1:5000, Proteintech, Cat. No. 81115-1-RR, RRID: AB_2923704). The membranes were then washed three times with TBST before being incubated for 40 min at room temperature with horseradish peroxidase-conjugated secondary antibodies. Subsequently, the membranes were washed three times with TBST, and were then exposed to a chemiluminescence reagent (TianGen, Beijing, China, PA112-02). Finally, ImageJ software (National Institutes of Health, Bethesda, MD, USA) was used to analyse the grey values of bands.

RNA sequencing (RNA-seq) analysis

Total hippocampal RNA was extracted using an RNA extraction kit (TianGen, Cat. No. DP419) according to the manufacturer's instructions. Using a 2100 Bioanalyzer system (Agilent, Santa Clara, CA, USA), RNA with an RNA integrity number > 9.0 was subjected to RNA sequencing library preparation using the RNA Library Prep Kit (TianGen, Cat. No. NR102). The library was then subjected to paired-end sequencing using next-generation sequencing based on the HiSeq sequencing platform (Illumina, San Diego, CA, USA). Differential gene expression was then tested using DESeq (Bioconductor version 3.10). Genes that had an expression |log2 fold change| ≥ 1 and adjusted *p*-value < 0.05 were used for the subsequent analysis.

Quantitative real-time polymerase chain reaction (qPCR)

TRIzol (TianGen, Cat. No. DP424) was used according to the manufacturer's protocol to extract total RNA from the mouse hippocampus and BV2 cells. A NanoDrop 2000 (Thermo Fisher Scientific) was used to detect the concentration and purity of the total RNA. The RNA was reverse-transcribed into cDNA using a FastKing 1 st Strand cDNA Synthesis Kit (TianGen, Cat. No. KR116) according to the manufacturer's instructions. SYBR Green Talent qPCR PreMix (TianGen, Cat. No. FP209) was used to perform qPCR according to the following steps: 95℃ for 3 min, followed by 40 cycles of 95℃ for 5 s and 60℃ for 15 s. Relative Gene expression was calculated using the $2^{-\Delta\Delta Ct}$ method with β-actin as the internal control. The primer sequences are listed in Table 1.

Enzyme-linked immunosorbent assay (ELISA)

Following the manufacturer's instructions, the CCK ELISA kit (RayBiotech, Atlanta, GA, USA, Cat. No. EIAM-CCK-1) was used to detect CCK concentrations in the mouse hippocampus. TNF-α (Boster, Cat. No. EK0527), IL-1β (Boster, Cat. No. EK0394), IL-6 (Boster, Cat. No. EK0411), IL-10 (Boster, Cat. No. EK0417) and

Table 1 Primer sequences for quantitative real-time polymerase chain reaction

ID	Forward (5′–3′)	Reverse (5′–3′)
β-actin	GTACCACCATGTACCCAGGC	AACGCAGCTCAGTAACAGTCC
C1qa	ACTGAAGGGCGT-GAAAGGCAAT	TTCTGGTATGGACTCTCCTG-GTTGG
C1qb	GCTAGAGCAAGAGGAGGTT-GTTCAC	TCAGGGAAAAGCAGAAAGC-CAGTG
C1qc	TGCCTGCTGCTGCT-GTTTCTTC	AGTCCATCATGCCCGTCCTTCC

MCP-1 (Boster, Cat. No. EK0568) ELISA kit were used to detect the levels of corresponding cytokines in the mouse serum.

Immunofluorescence

Mice were deeply anaesthetised with sevoflurane and fixed on an operating table. Cold phosphate-buffered saline (PBS) was perfused transcardially. Once the fluid from the auricula extra had cleared, 4% paraformaldehyde was used for perfusion. The brain was then isolated from the skull and placed in 4% paraformaldehyde for 24 h, followed by dehydration for 48 h in 30% sucrose solution. Next, the brains were coronally sectioned at 35 μm using a cryostat microtome (Leica, Wetzlar, Germany, CM3050S). The sections were then washed three times with PBS and blocked in 10% normal goat serum with 0.3% Triton for 1 h at 37℃. Subsequently, the sections were incubated overnight at 4℃ with the following primary antibodies: mouse anti-PSD95 (1:100, Cell Signaling Technology, Cat. No. 36233, RRID: AB_2721262), rabbit anti-vGlut1 (1:100, Abcam, Cat. No. ab227805, RRID: AB_2868428), rabbit anti-c-Fos (1:500, Cell Signaling Technology, Cat. No. #2250, RRID: AB_2247211), chicken anti-GFAP (1:1000, Abcam, Cat. No. ab4674, RRID: AB_304558), rabbit anti-C1q (1:200, Abcam, Cat. No. ab182451, RRID: AB_2732849), rabbit anti-ionized calcium-binding adapter molecule 1 (Iba1; 1:500, Wako, Richmond, VA, USA, Cat. No. 019-19741, RRID: AB_839504), chicken anti-Iba1 (1:500, HUABIO, Cat. No. HA601376) and rabbit anti-C3 (1:50, Proteintech, Cat. No. 21337-1-AP, RRID: AB_2878843). After three washes with PBS, the sections were incubated with fluorescent secondary antibodies for 50 min at 37℃, followed by staining with 4′,6-diamidino-2-phenylindole for 10 min at 37℃. A confocal fluorescence microscope (ZEISS, Oberkochen, Germany) was used to photograph the brain sections, and ZEN 3.3 (blue edition) software was used to process and analyse the data. The Imaris software (version 10.1, Oxford Instruments) was used to analyse the morphology and 3D reconstruction of microglia.

Electrophysiological recordings

Similar to our previous studies [24, 25], in vitro whole-cell recordings from dorsal hippocampal CA1 excitatory neurons were used to examine synaptic transmission after CCK8 treatment. First, each mouse was deeply anaesthetised with pentobarbital sodium (50 mg/kg, intraperitoneally) and sacrificed. After removing the skull, the brain was immediately immersed in cold oxygenated cutting solution and coronally sectioned at 300 μm using a vibratome (Leica, VT1200S). Slices were then transferred to oxygenated artificial cerebrospinal fluid (ACSF) for at least 1 h at 30℃. The ACSF included (in mM): 125.0 NaCl, 1.2 NaH_2PO_4, 26.0 $NaHCO_3$, 5.0 KCl, 2.6 $CaCl_2$, 1.3 $MgCl_2$, and 10.0 glucose (pH 7.3–7.4, 305 mOsm/kg). For recording, an individual slice was placed in the submersion-recording chamber and continuously perfused with ACSF (2 mL/min). Only one neuron was recorded in each slice.

An Axonpatch 700B Amplifier, a Digidata 1500B Digital Converter, and pClamp 10 software (all Molecular Devices, San Jose, CA, USA) were used to obtain and analyse the electrical signals. The recording pipettes (World Precision Instruments, Sarasota, FL, USA, 4–7 MΩ) were filled with an internal solution containing (in mM): 122.0 potassium-gluconate, 2.0 $MgCl_2$, 0.3 $CaCl_2$, 5.0 NaCl, 5.0 EGTA, 10.0 HEPES, 4.0 Mg-ATP, and 0.3 Na_3-GTP (pH 7.3–7.4, 300 mOsm/kg). Spontaneous excitatory postsynaptic currents (sEPSCs) were recorded at −70 mV with picrotoxin (50 μM), and 1 mM tetrodotoxin was then added to record miniature excitatory postsynaptic currents (mEPSCs). Traces of a fixed length (5 min) were analysed using pClamp 10 software.

Statistical analysis

A website (www.randomization.com) was used to perform the randomisation of each group of animals or cells. The animal and cell interventions, data collection, and data analyses were blinded using different experimenters. Similar to our previous studies, statistical power analysis was used to allow significant differences with respect to sample sizes (GPower 3, ≥ 0.8 for sufficient power validation) [8, 26].

Prism 7.0 (GraphPad, Boston, MA, USA) was used for the statistical analyses, and data normality was assessed using the Shapiro–Wilk test. Quantitative data are expressed as the mean ± standard deviation (SD). Student's *t*-test was used to compare differences between two groups. One-way or two-way analysis of variance (ANOVA) was used for more than two groups, followed by Bonferroni *post hoc* test. Repeated measures ANOVA was used to analyse the data from repeated measurements, followed by Bonferroni *post hoc* test. A p-value < 0.05 was considered significant.

Results

Cognitive dysfunction is accompanied by reduced hippocampal CCK and excitatory synapses in SAE model mice

The experimental timeline is shown in Fig. 1A. Compared with mice in the control group, LPS-injected mice had increased serum cytokine levels (TNF-α, IL-1β, IL-6, IL-10 and MCP-1) at 3 and 6 h (Fig. 1B-F), higher sepsis scores on days 1–3 after injection (Fig. 1G) and lower body weights on days 1–4 after injection (Fig. 1H). These data indicate that 5 mg/kg LPS injection can be successfully used to construct a sepsis model in mice.

The FCT context test and MWM reflect hippocampus-dependent memory, whereas the FCT tone test reflects hippocampus-independent memory in rodents [27, 28]. In the training phase of the FCT, there was no significant

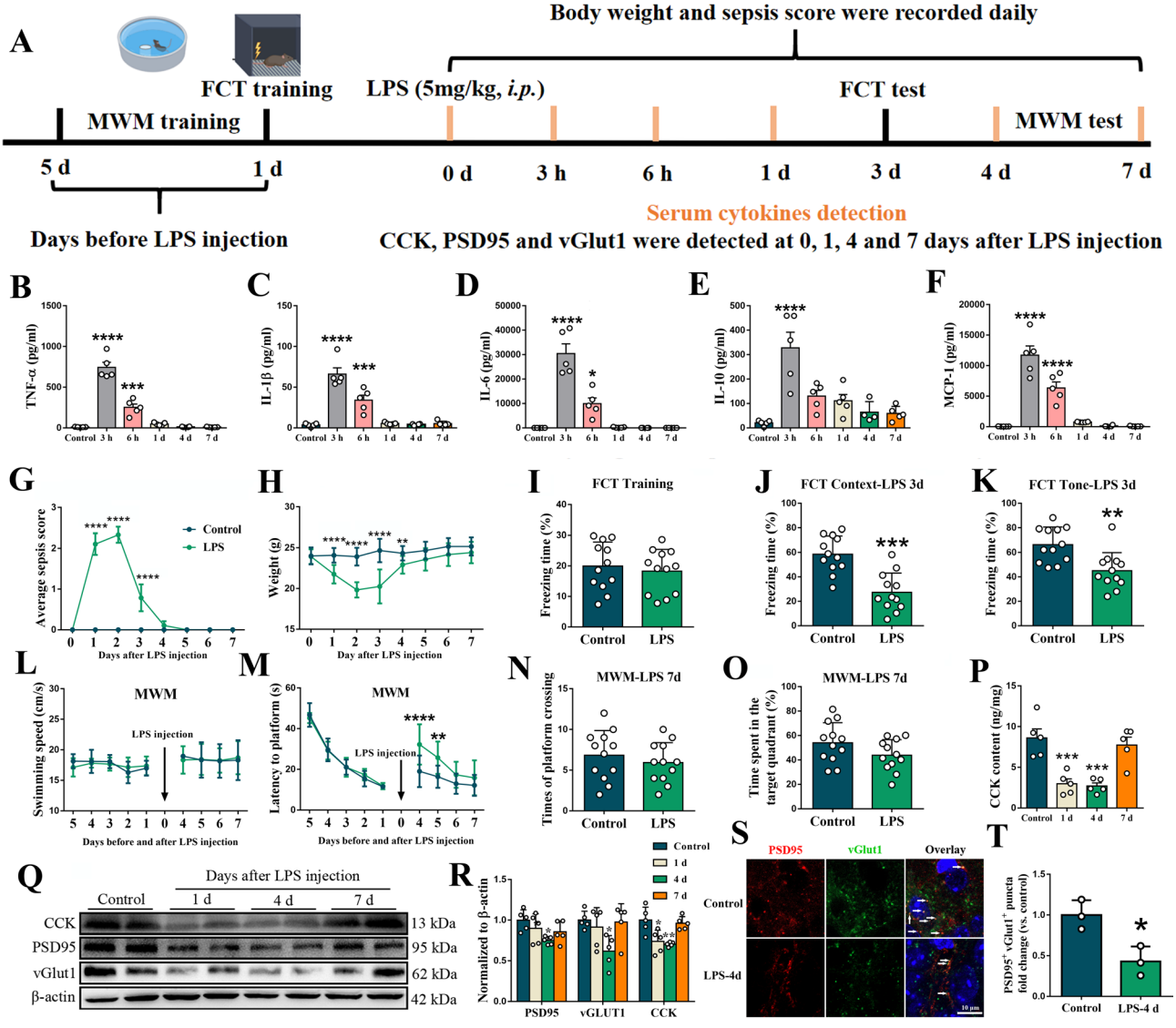

Fig. 1 Cognitive dysfunction is accompanied by reduced hippocampal cholecystokinin (CCK) and excitatory synapses in sepsis-associated encephalopathy (SAE) model mice. (A) Experimental timeline. ELISA was performed to detect the serum levels of TNF-α (B), IL-1β (C), IL-6 (D), IL-10 (E) and MCP-1 (F), and hippocampal CCK concentration (P). (G) Daily sepsis scores of control mice and mice after lipopolysaccharide (LPS) injection. (H) Daily body weights of control mice and mice after LPS injection. The percentages of freezing time in the (I) training phase, (J) context test, and (K) tone test were recorded on day 1 before and day 3 after the LPS injection. (L) Swimming speed and (M) latency to the platform were recorded in the training and place navigation tests. (N) The number of platform crossings and (O) time spent in the target quadrant were recorded in the Morris Water Maze (MWM) spatial probe test on day 7 after LPS injection. (Q, R) Protein levels of CCK, PSD95, and vGlut1 were detected by western blot. (S, T) Immunofluorescence was used to detect the number of excitatory synapses (white arrows) in the dorsal hippocampal CA1 region. Data are expressed as the mean ± SD (n = 12 per group for behavioural tests; n = 3-5 per group for ELISA, immunofluorescence and western blot). Data B-F, P and R were analysed by one-way ANOVA followed by Bonferroni *post hoc* test; data G, H, L and M were analysed by repeated measures ANOVA followed by Bonferroni *post hoc* test; data I-K, N and O were analysed by student's *t*-test. *$p < 0.05$, **$p < 0.01$, ***$p < 0.001$, ****$p < 0.0001$ vs. control group

difference in the percentage of freezing time between mice in the control and LPS groups (Fig. 1I). However, compared with the control mice, the percentage of freezing time was lower in LPS-injected mice on day 3 after injection in both the context and tone tests (Fig. 1J, K), indicating both hippocampal- and non-hippocampal-dependent fear memory impairments on day 3 after LPS injection.

In the MWM, there was no significant difference in swimming speed between mice in the control and LPS groups (Fig. 1L), indicating that SAE model mice had normal locomotor activity. Compared with mice in the control group, the latency to the platform was longer in LPS-injected mice on days 4 and 5 after injection (Fig. 1M). However, there were no significant differences in the number of platform crossings or time spent in the target quadrant between mice in the control and LPS groups (Fig. 1N, O), indicating that cognitive function recovered on day 7 in the SAE model mice. Together, these findings indicate that a model of cognitive dysfunction was established successfully in the SAE model mice.

Both ELISA and western blot results revealed a decrease in hippocampal CCK protein levels on days 1 and 4 after LPS injection relative to control mice (Fig. 1P-R). Moreover, compared with mice in the control group, the protein levels of PSD95 and vGlut1 (Fig. 1Q, R) and the number of excitatory synapses in the dorsal hippocampal CA1 region (Fig. 1S, T) were lower on day 4 after LPS injection. Together, these results suggest that decreased CCK and excitatory synapses accompany cognitive dysfunction in SAE model mice.

Dorsal hippocampal CA1 region CCK8 injection ameliorates cognitive dysfunction in SAE model mice

The cannula implantation site and experimental timeline are shown in Fig. 2A. Because previous studies have demonstrated that CCK enhances cognition [29], we explored the effects of different doses of CCK8 (2, 10, and 50 ng) on cognitive function in SAE model mice.

In the training phase of FCT, there were no significant differences in the percentage of freezing time among the five groups (Fig. 2B). Both 10 and 50 ng CCK8 increased the percentage of freezing time in SAE model mice in the context test (Fig. 2C) but not in the tone test (Fig. 2D). Furthermore, there were no significant differences in swimming speed (Fig. 2E) or latency to the platform (Fig. 2F) among the five groups in the MWM training phase. In the MWM spatial navigation test, there were no significant differences in swimming speed among the five groups (Fig. 2G), indicating that 2, 10, or 50 ng CCK8 injection does not affect the locomotor ability of mice. However, 10 ng CCK8 injection decreased the latency to the platform and increased both the number of platform crossings and time spent in the target quadrant. Furthermore, 50 ng CCK8 injection reduced the latency to the platform and increased the time spent in the target quadrant of LPS-exposed mice (Fig. 2H–K).

CCK8 ameliorates excitatory synaptic plasticity in the dorsal hippocampal CA1 of SAE model mice

The experimental timeline is shown in Fig. 3A. Because both 10 ng and 50 ng CCK8 improved cognitive dysfunction in SAE model mice, we chose 10 ng CCK8 for the follow-up experiments. We hypothesised that CCK8 may ameliorate cognitive dysfunction by modulating synaptic plasticity; we therefore detected the effects of CCK8 on the number and function of synapses in dorsal hippocampal CA1 excitatory neurons. CCK8 increased the PSD95 and vGlut1 protein levels (Fig. 3B, C) as well as the number of excitatory synapses (Fig. 3D, E) in the dorsal hippocampal CA1 region of SAE model mice. These findings suggest that CCK8 may ameliorate cognitive dysfunction in SAE model mice by increasing the number of excitatory synapses. To explore the effects of CCK8 on glutamatergic transmission, whole-cell patch clamping was performed to record sEPSCs of excitatory neurons in dorsal hippocampal slices. CCK8 significantly increased the frequency of sEPSCs in dorsal hippocampal CA1 excitatory neurons of SAE model mice (Fig. 3F–H). In addition, we recorded mEPSCs to assess single synaptic responses to individual synaptic vesicles. The frequency of mEPSCs was significantly increased in SAE model mice after CCK8 injection (Fig. 3I–K). Together, these results indicate that CCK8 can ameliorate glutamatergic transmission impairments.

CCK8 inhibits C1q-mediated microglial phagocytosis of synapses and A1 astrocyte polarisation

The experimental timeline is shown in Fig. 4A. We used RNA sequencing to explore the potential targets of CCK8 in the regulation of excitatory synaptic plasticity. Compared with the LPS group, 26 Genes were upregulated in the control group and 39 genes were upregulated in the LPS + CCK8 group. There was no overlap between the two sets of different genes (Fig. 4B). However, of the 201 Genes that were downregulated in the control group and the 94 genes that were downregulated in the LPS + CCK8 group compared with the LPS group, there were 82 genes in common (Fig. 4B). The 10 genes with the most significant changes are presented in a heatmap (Fig. 4B), and include the *C1qa*, *C1qb*, and *C1qc* isoforms of *C1q*, which have been suggested to be associated with synaptic plasticity [30]. We therefore postulated that CCK8 might regulate synaptic plasticity and cognitive function by suppressing C1q expression in SAE model mice. Our western blot and qPCR results were consistent with the RNA sequencing findings, and supported our assumption (Fig. 4C–E).

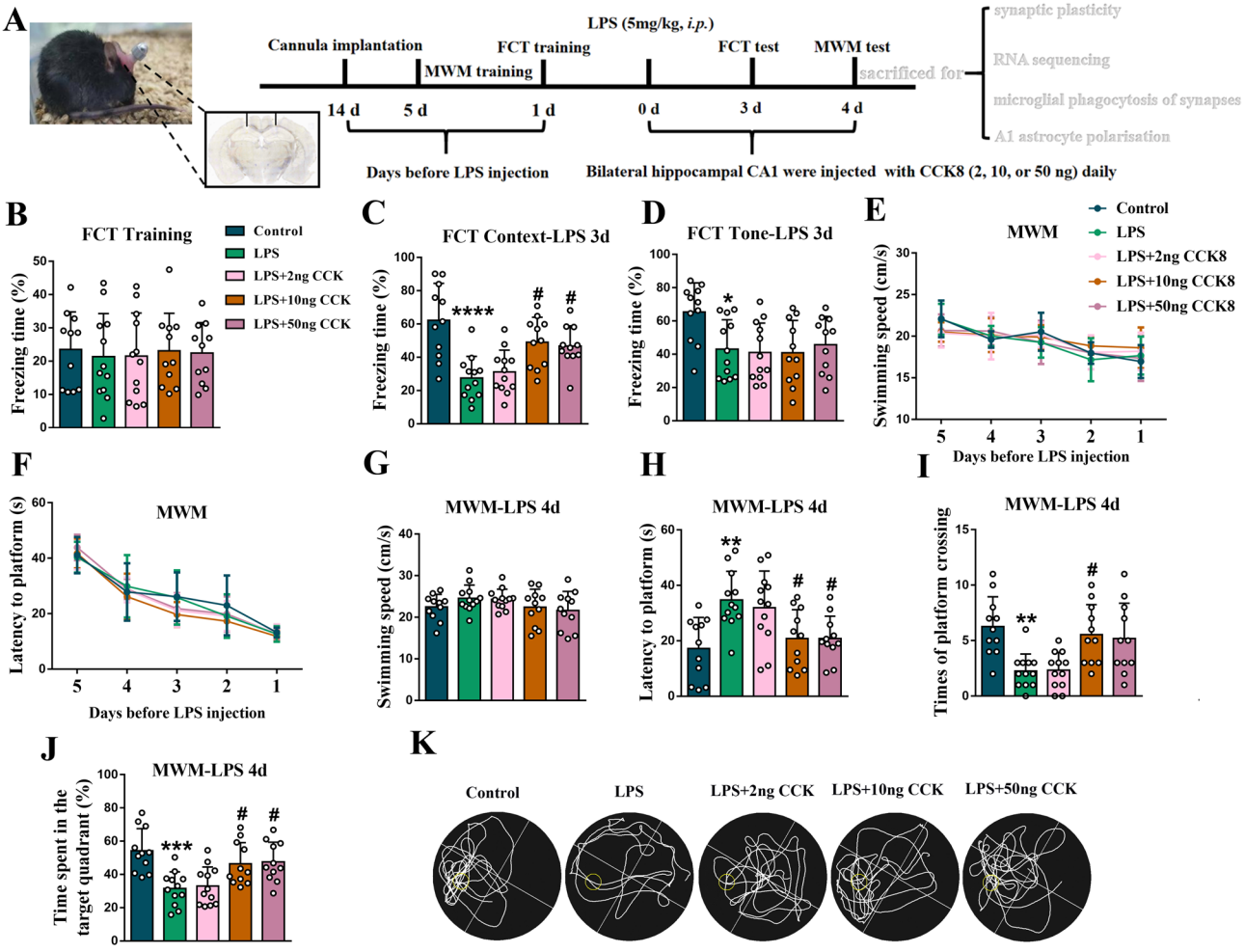

Fig. 2 Dorsal hippocampal CA1 region CCK8 injection ameliorates cognitive dysfunction in SAE model mice. (A) Cannula implantation site and experimental timeline. The percentages of freezing time in the (B) training phase, (C) context test, and (D) tone test were recorded on day 3 after LPS injection. (E) Swimming speed and (F) escape latency were recorded in the training phase. (G) Swimming speed, (H) latency to the platform, (I) number of platform crossings, and (J) time spent in the target quadrant were recorded in the MWM spatial probe test on day 4 after LPS injection. (K) Swimming trajectories. Data are expressed as the mean ± SD ($n = 11–12$ per group). Data B-D and G-J were analysed by two-way ANOVA followed by Bonferroni *post hoc* test; data E and F were analysed by repeated measures ANOVA followed by Bonferroni *post hoc* test. *$p < 0.05$, **$p < 0.01$, ***$p < 0.001$, ****$p < 0.0001$ vs. control group; $^{\#}p < 0.05$ vs. LPS group

It is thought that C1q-labeled synapses result in microglial phagocytosis, which may be a driver of synaptic loss [31]. The number of C1q-labeled synapses (C1q colocalised with PSD95) phagocytosed by microglia were increased in the dorsal hippocampus CA1 region of SAE model mice compared with control mice, while these changes were reversed by CCK8 injection, suggesting that CCK8 can inhibit the C1q-mediated microglial phagocytosis of synapses (Fig. 4F, J). In addition, CCK8 significantly inhibited microglial activation, as evidenced by reduced microglial fluorescence intensity and soma volume, and increased branch length compared to SAE mice (Fig. 4F-I). Together, these results indicate that CCK8 inhibited microglial activation, while enhancing synaptic plasticity in the dorsal hippocampal CA1 region by inhibiting microglial C1q expression.

Previous studies have demonstrated that C1q can induce the polarisation of A1 astrocytes, thereby indirectly impairing synaptic plasticity [8, 32]. We therefore detected the number of A1 astrocytes in the dorsal hippocampal CA1 region. The protein levels of the A1 astrocyte marker C3 and the astrocyte marker GFAP (Fig. 4M, N) were both increased in LPS-injected mice compared with control mice, and there was increased colocalization of the two markers. However, these phenomena were reversed by CCK8 injection (Fig. 4K, L). Together, these findings suggest that C1q-induced A1 astrocyte polarisation may be another mechanism underlying synaptic plasticity impairments.

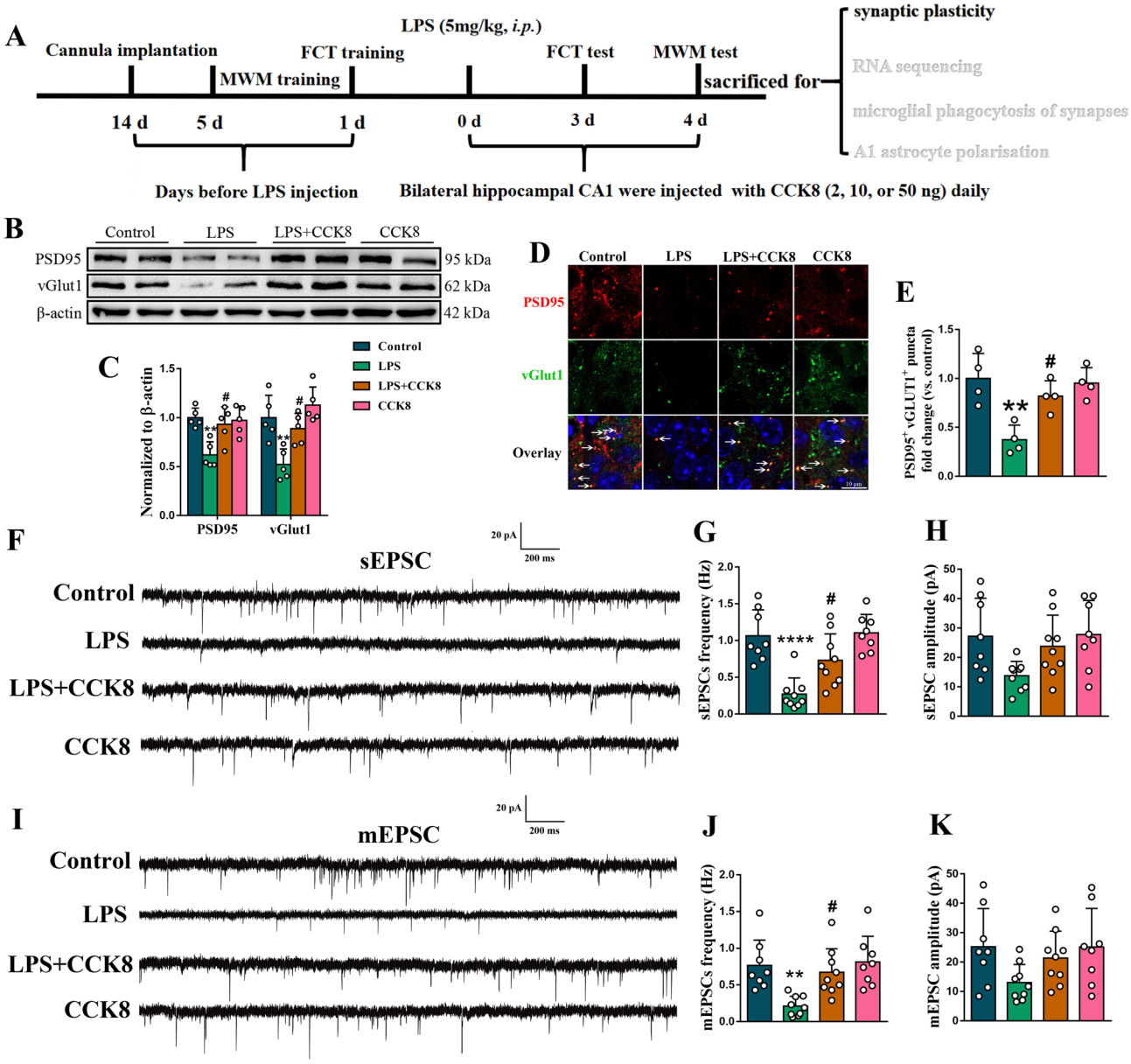

Fig. 3 CCK8 ameliorates excitatory synaptic plasticity in the dorsal hippocampal CA1 region of SAE model mice. (A) Experimental timeline. (B, C) Western blot was used to detect the hippocampal protein levels of PSD95 and vGlut1 in mice. (D, E) Immunofluorescence was used to detect the numbers of excitatory synapses (white arrows) in the dorsal hippocampal CA1 region. (F) Representative traces for sEPSCs. Statistical results of (G) sEPSC frequency and (H) amplitude. (I) Representative traces for mEPSCs. Statistical results of (J) mEPSC frequency and (K) amplitude. Data are expressed as the mean ± SD ($n = 4$–5 per group). All data were analysed by two-way ANOVA followed by Bonferroni *post hoc* test. $^{**}p < 0.01$, $^{****}p < 0.0001$ vs. control group; $^{\#}p < 0.05$ vs. LPS group

Activation of CCK-positive neurons ameliorates cognitive dysfunction in SAE model mice

Previous studies have demonstrated that the activation of CCK-positive neurons in the hippocampal DG region can induce CCK release [33]. To evaluate whether the activation of CCK-positive neurons in the dorsal hippocampal CA1 region might play a role in the cognitive dysfunction of LPS-exposed mice by releasing CCK, a chemogenetic approach (CCK-Cre mice received an injection of AAV-Ef1α-DIO-hM3Dq-mCherry or AAV-Ef1α-DIO-mCherry into the dorsal hippocampal CA1) was used to activate CCK-positive neurons. The activation of CCK-positive neurons led to the release of CCK and other neurotransmitters, and CCK2R is the primary receptor for CCK in the CNS [33, 34]. We therefore used the CCK2R antagonist L365,260 to explore whether CCK released by CCK-positive neurons plays a role in the observed effects. The AAV injection site and experimental timeline are shown in Fig. 5A.

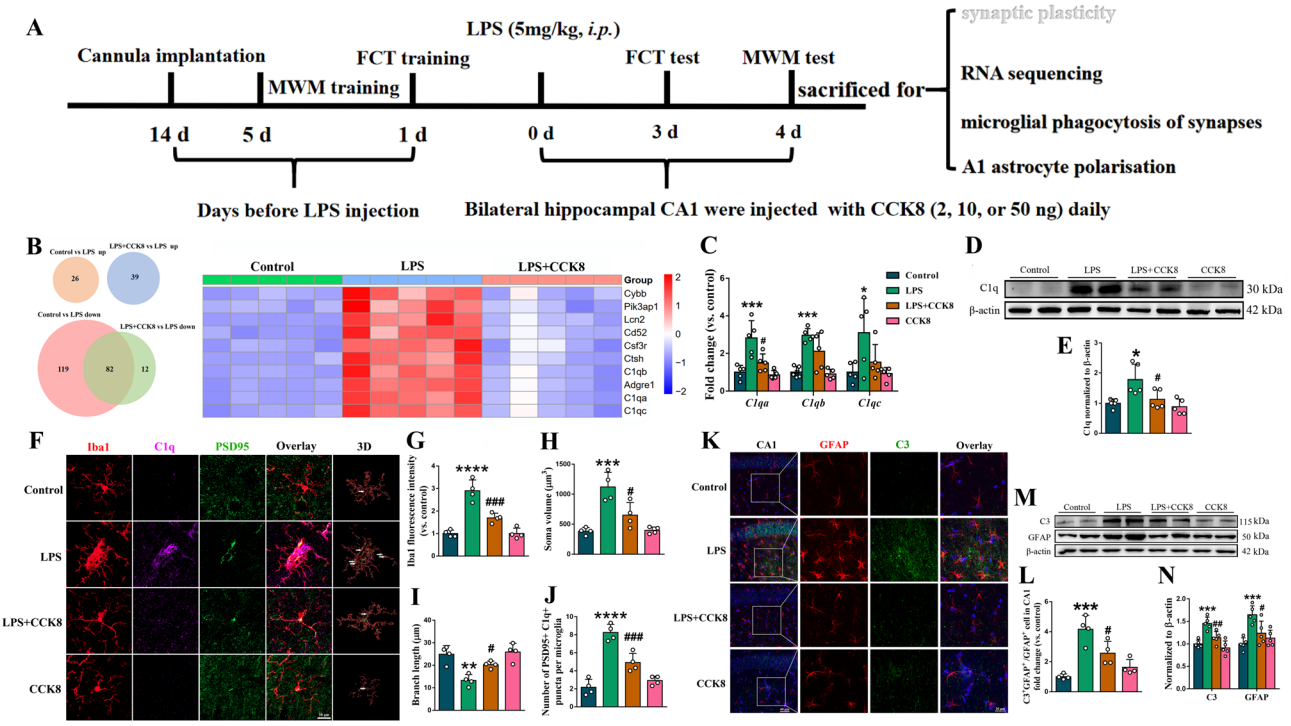

Fig. 4 CCK8 inhibits C1q-mediated microglial phagocytosis of synapses and A1 astrocyte polarisation in SAE model mice. (A) Experimental timeline. (B) Venn diagram and heatmap showing differentially expressed genes in the control and LPS + CCK8 groups compared with the LPS group. (C) mRNA and (D, E) protein levels of C1q were detected by qPCR and western blot, respectively. Immunofluorescence was used to detect the number of $PSD95^{+}C1q^{+}$ with microglia (F, J), Iba1 fluorescence intensity (G), soma volume (H), branch length (I) and the colocalization of (K, L) GFAP with C3 in the dorsal hippocampal CA1 region of mice. (M, N) Western blot was used to detect GFAP and C3 protein levels in the hippocampus of mice. Data are expressed as the mean ± SD ($n = 4$–5 per group). All data were analysed by two-way ANOVA followed by Bonferroni *post hoc* test. $^{*}p < 0.05$, $^{**}p < 0.01$, $^{***}p < 0.001$, $^{****}p < 0.0001$ vs. control group; $^{\#}p < 0.05$, $^{\#\#}p < 0.01$, $^{\#\#\#}p < 0.001$ vs. LPS group

In the training phase of FCT, there were no significant differences in the percentage of freezing time among the four groups (Fig. 5B). The activation of CCK-positive neurons increased the percentage of freezing time of SAE model mice in the context test but not the tone test. However, L365,260 blocked the effects of CCK-positive neuronal activation (Fig. 5C, D). In the MWM training phase, the four groups had no significant differences in swimming speed (Fig. 5E) or latency to the platform (Fig. 5F). Similarly, in the place navigation test of MWM, there were no significant differences in swimming speed among the four groups (Fig. 5G). The activation of CCK-positive neurons decreased the latency to the platform and increased both the platform crossings and time spent in the target quadrant of SAE model mice, and L365,260 blocked the effects of CCK-positive neuronal activation (Fig. 5H–K).

Activation of CCK-positive neurons inhibits the C1q-mediated microglial phagocytosis of synapses

SAE model mice with AAV-Ef1α-DIO-hM3Dq-mCherry injection had more c-Fos-positive cells in the dorsal hippocampal CA1 region than mice with AAV-Ef1α-DIO-mCherry injection (Fig. 5L, M). These results suggest that the designer receptors exclusively activated by designer drugs approach can effectively activate CCK-positive neurons in the dorsal hippocampal CA1 region of LPS-exposed mice. Furthermore, there was no significant difference in c-Fos-positive cell number between AAV-Ef1α-DIO-hM3Dq-mCherry + L365,260 (hM3Dq + L) group and AAV-Ef1α-DIO-hM3Dq-mCherry (hM3Dq) group (Fig. 5L, M). This finding indicates that L365,260 injection does not affect the activity of CCK-positive neurons.

To confirm whether CCK-positive neuronal activation has a similar effect to that of CCK8 injection, we investigated the C1q-mediated microglial phagocytosis of synapses. CCK-positive neuronal activation inhibited the total hippocampal protein levels of C1q (Fig. 5N, O). Furthermore, CCK-positive neuronal activation inhibited microglia activation and C1q-mediated microglial phagocytosis of synapses, similar to CCK8 injection (Fig. 5P, T), while L365,260 was able to block the effects of CCK-positive neuronal activation (Fig. 5N-T).

CCK8 inhibits C1q expression via CCK2R in BV2 microglia

The experimental timeline is shown in Fig. 6A. Because C1q was produced by microglia in the CNS, the BV2

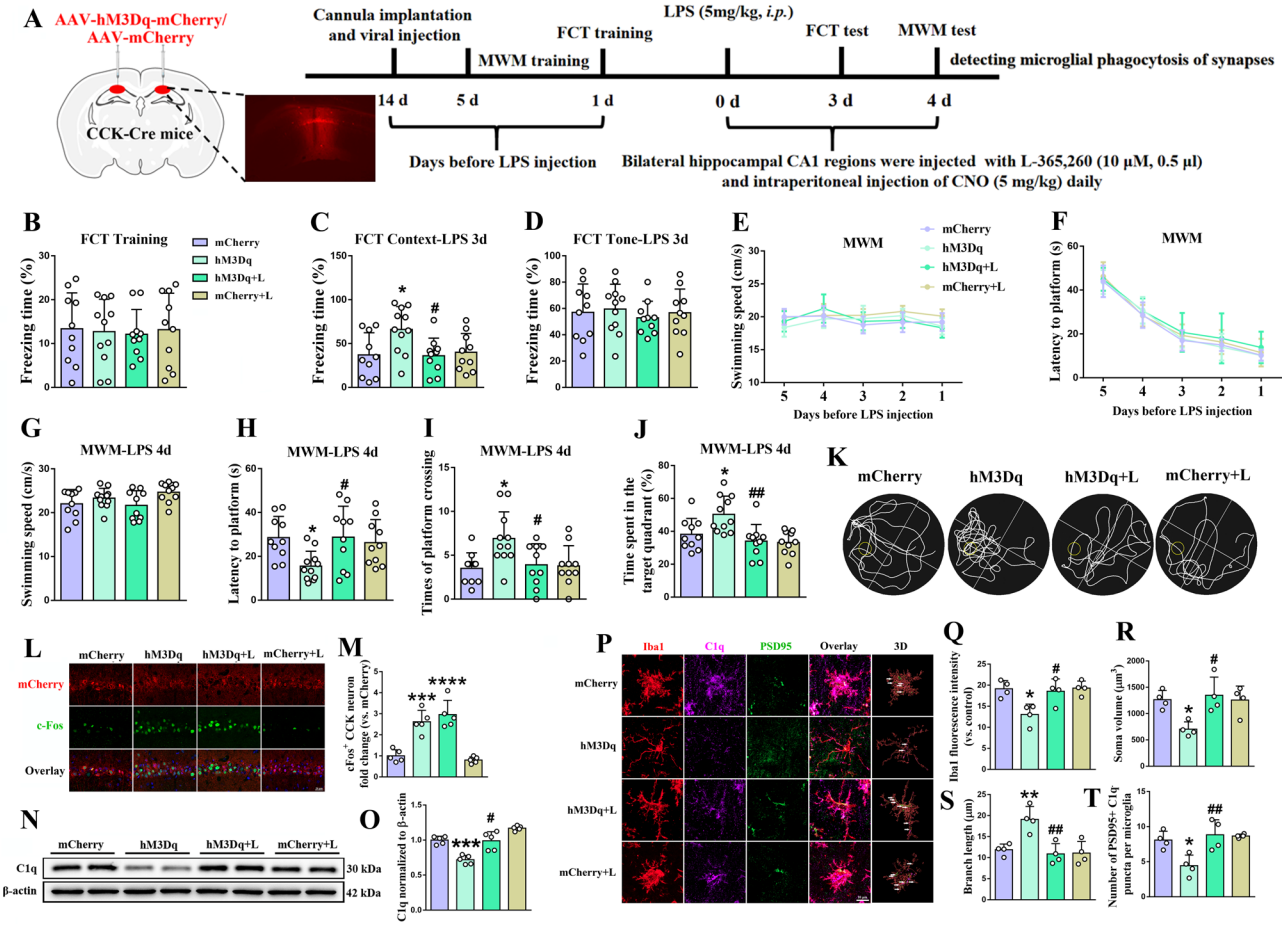

Fig. 5 Activation of CCK-positive neurons in the dorsal hippocampal CA1 region ameliorates cognitive dysfunction and inhibits the C1q-mediated microglial phagocytosis of synapses in SAE model mice. (A) AAV injection site and experimental timeline. The percentages of freezing time in the (B) training phase, (C) context test, and (D) tone test were recorded on day 3 after LPS injection. (E) Swimming speed and (F) escape latency were recorded in the training phase. (G) Swimming speed, (H) latency to the platform, (I) number of platform crossings, and (J) time spent in the target quadrant were recorded in the MWM spatial probe test on day 4 after LPS injection. (K) Swimming trajectories. Immunofluorescence was used to detect the colocalization of mCherry with c-Fos (L, M), and the number of PSD95^{+}C1q^{+} with microglia (P, T), Iba1 fluorescence intensity (Q), soma volume (R) and branch length (S). (N, O) Western blot was used to detect the mice hippocampal protein levels of C1q. Data are expressed as the mean ± SD ($n = 11–12$ per group for behavioural tests; $n = 3–5$ per group for immunofluorescence and western blot). Data E and F were analysed by repeated measures ANOVA followed by Bonferroni *post hoc* test, the remaining data were analysed by two-way ANOVA followed by Bonferroni *post hoc* test. *$p < 0.05$, **$p < 0.01$ ***$p < 0.001$, ****$p < 0.0001$ vs. mCherry group; $^{\#}p < 0.05$, $^{\#\#}p < 0.01$ vs. hM3Dq group

cell line was used to establish the in vitro SAE model. We observed C1q protein levels to determine the optimal concentration and duration for LPS exposure in BV2 cells. First, BV2 microglia were exposed to different concentrations of LPS (0.1, 0.2, 0.5, 1, and 2 μg/mL) for 6 h. Both 1 and 2 μg/mL LPS exposure increased C1q protein levels in the medium and in cells (Fig. 6B, C). We therefore exposed BV2 cells to 1 μg/mL LPS for 1, 3, 6, 12, and 24 h; LPS exposure for 6, 12, and 24 h increased C1q expression (Fig. 6D, E). Ultimately, 1 μg/mL LPS exposure for 6 h was selected to construct the in vitro SAE model in BV2 cells.

Different concentrations of CCK8 were then used to treat LPS-exposed BV2 cells. Both 1 and 2 μM of CCK8 were able to inhibit the intracellular and medium levels of C1q (Fig. 6F, G). Moreover, the different concentrations of CCK8 did not affect BV2 cell viability (Fig. 6H). Next, the CCK2 antagonist L365,260 was used to confirm that CCK8 acts through microglial CCK2R. Indeed, L365,260 blocked the CCK8-induced inhibition of C1q expression in BV2 cells (Fig. 6I, J). In addition, the CCK1R antagonist SR27897 was used to confirm the lack of a role for CCK1R in these effects; as expected, SR27897 did not block the CCK8-induced inhibition of C1q expression (Fig. 6K, L).

Discussion

The present study aimed to evaluate the roles of CCK8 and CCK-positive neurons of the hippocampal CA1 region in enhancing synaptic plasticity and alleviating

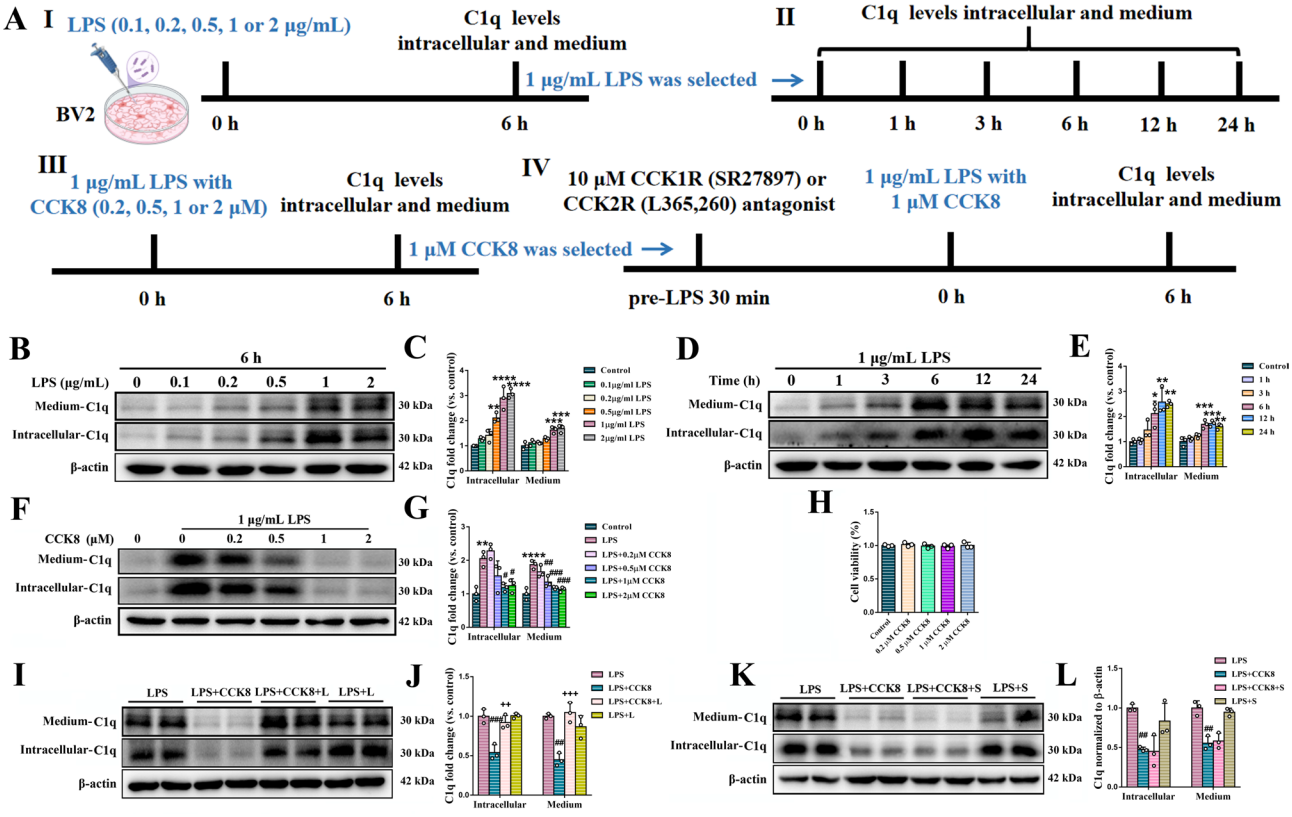

Fig. 6 CCK8 inhibits C1q expression via CCK2R in BV2 microglia. (A) Experimental timeline. (B–G, I–L) Western blot was used to detect C1q protein levels in the medium and in cells. (H) A Cell Counting Kit-8 was used to detect cell viability. Data are expressed as the mean ± SD ($n = 3$ per group). Data B-E and H were analysed by one-way ANOVA followed by Bonferroni *post hoc* test, the remaining data were analysed by two-way ANOVA followed by Bonferroni *post hoc* test. $^{*}p < 0.05$, $^{**}p < 0.01$, $^{***}p < 0.001$, $^{****}p < 0.0001$ vs. control group; $^{\#}p < 0.05$, $^{\#\#}p < 0.01$, $^{\#\#\#}p < 0.001$ vs. LPS group; $^{++}p < 0.01$, $^{+++}p < 0.001$ vs. LPS + CCK8 group

cognitive impairments in SAE model mice. In our in vivo experiments, CCK levels and excitatory synapse numbers in the hippocampus were significantly decreased in a mouse model of SAE. Moreover, CCK8 supplementation or the activation of CCK-positive neurons in the hippocampal CA1 region was able to inhibit the C1q-mediated microglial phagocytosis of synapses and the A1 polarisation of astrocytes, thereby improving synaptic plasticity and cognitive impairments in SAE model mice. In the in vitro experiments, CCK8 inhibited C1q expression via CCK2R in LPS-stimulated BV2 cells. Together, these data indicate the crucial role of CCK8 and CCK-positive neurons of the hippocampal CA1 region in enhancing SAE-induced synaptic plasticity and alleviating cognitive impairments in mice. Notably, the results of the present study demonstrate the important effects of CCK8 and CCK-positive neurons on synaptic plasticity and cognitive impairments in the context of SAE (Fig. 7).

Intraperitoneal LPS injection and cecum Ligation and puncture are two common ways to construct sepsis models in animals. Compared with cecum Ligation and puncture, intraperitoneal LPS injection has the advantage of being simple to model and having high reproducibility while simulating the pathophysiology of sepsis. In accordance with previous studies, 5 mg/kg LPS intraperitoneal injection was used in the present study to construct the sepsis mouse model [4]. Our LPS-injected mice had significantly higher serum cytokine levels and sepsis scores than control mice, indicating the successful establishment of the sepsis model. In addition, MWM and FCT results demonstrated that our sepsis mice had cognitive impairment. Taken together, our findings indicate that an SAE model with cognitive impairment was successfully established in mice.

Neuropeptides are the most diverse signalling molecules of the mammalian brain and involve many physiological functions, such as cognition, sleep–awake cycles, and pain [35–37]. Substance P, calcitonin gene-related peptide, neuropeptide Y, vasoactive intestinal polypeptide, and somatostatin are other well-known neuropeptides; however, CCK is one of the earliest identified and most abundant neuropeptides in the brain [38]. In the present study, hippocampal CCK levels were significantly decreased in SAE model mice. An analysis of biomarkers revealed that higher cerebrospinal fluid levels of CCK are associated with higher memory-related scores

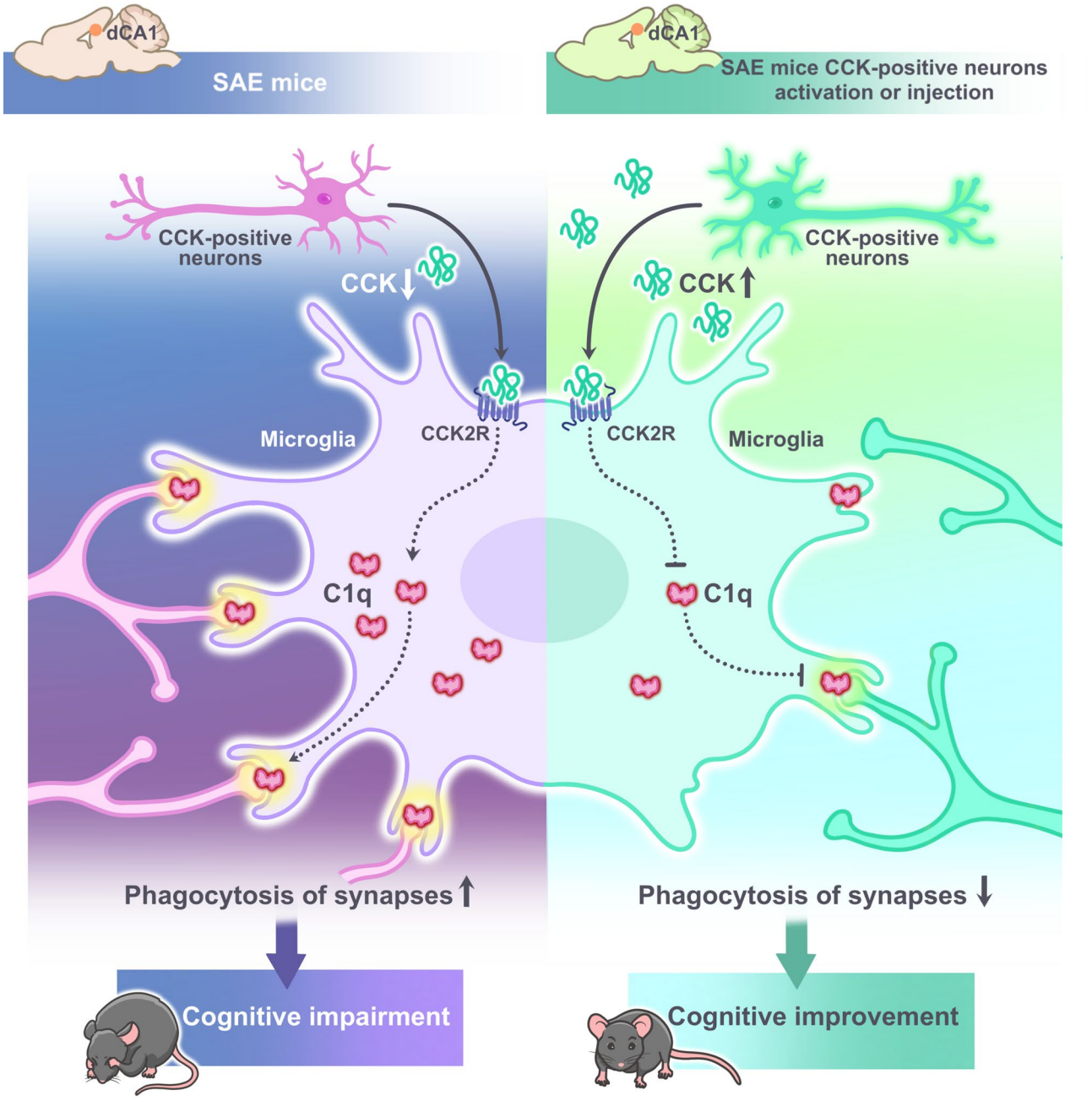

Fig. 7 Schematic diagram of the mechanism by which CCK improves cognitive function by inhibiting C1q-mediated microglial phagocytosis of synapses in SAE mice

and lower chances of developing mild cognitive impairment or Alzheimer's disease [7]. CCK is also significantly decreased in an APP/PS1 mouse model of Alzheimer's disease, suggesting that CCK may be involved in the development of this disease [39]. In the present study, we further validated the role of CCK in cognitive impairment by supplementing exogenous CCK8 in the hippocampal CA1 region of our mouse model. CCK8 (10 and 50 ng) was able to alleviate hippocampus-dependent memory impairment but not hippocampus-independent (FCT tone test) memory impairment, which may be because CCK8 was injected into the CA1 region only, rather than via systemic administration.

Previous studies have revealed that the activation of CCK neurons in the hippocampal DG region promotes CCK release [33]. We therefore injected chemogenetic activation virus (AAV2/9-Ef1α-DIO-hM3Dq-mCherry-WPREs) into the hippocampal CA1 region of CCK-Cre mice, and achieved the activation of CCK neurons in the CA1 region via the intraperitoneal injection of clozapine

N-oxide. We thus investigated the effects of promoting endogenous CCK release on cognitive impairment in SAE model mice. Activation of CCK-positive neurons in the hippocampal CA1 region alleviated cognitive impairment in SAE model mice, similar to the effects observed with CCK8 injections. Although the receptors for the action of CCK are CCK1R and CCK2R, CCK2R is predominant in the CNS. Asrican et al. reported that the activation of CCK-positive neurons in the hippocampal DG region promotes the neurogenic proliferation of neural stem cells, and noted that these effects can be blocked by CCK2R antagonists [33]. Furthermore, Chen et al. demonstrated that high-frequency stimulation induces neocortical long-term potentiation by releasing CCK, whereas a CCK2R antagonist can block the role of CCK [29]. Similarly, the results of this study suggest that the effect of CCK-positive neurons activation on improving cognitive function in SAE mice can be blocked by CCK2R antagonist (L365,260), which rules out the possibility that CCK-positive neurons activation affects cognitive function in SAE mice through the release of other neurotransmitters. This provides a theoretical basis for future gene therapy to treat cognitive impairments in SAE.

Synapses are structures that are essential for signalling between neurons. The structural and functional integrity of hippocampal excitatory synapses plays a critical role in regulating learning and memory [40]. In the present study, SAE model mice had hippocampal CA1 excitatory synaptic loss, which is consistent with the findings of previous studies [41]. In addition, CCK8 increased the excitatory synapse number and the frequency and amplitude of EPSCs in the hippocampal CA1 region of SAE model mice, suggesting that CCK8 may improve cognition in these mice by enhancing synaptic plasticity. Similarly, Dehghani et al. reported that CCK8 positively affects hippocampal synaptic plasticity, and consequently cognitive function, in rats [42]. Moreover, CCK knockout mice have deficits in neocortical long-term potentiation and dysfunctions in cue–cue associative learning, and these effects can be rescued by the local injection of CCK [29]. These reports are consistent with the present findings, and suggest that CCK improves cognitive impairments in SAE model mice by attenuating excitatory synaptic plasticity damage.

In the current study, although we elucidated the role of CCK in cognitive impairment in SAE model mice, the molecular mechanisms by which CCK improves synaptic plasticity remain unclear. We thus performed RNA sequencing to screen for potential targets of CCK8. Notably, CCK8 significantly inhibited hippocampal C1q expression in the SAE model mice. C1q is produced by microglia in the CNS and is an initiating factor of the classical complement cascade [43]. Microglia clear away C1q-localised dysfunctional synapses via phagocytosis, which can provide space for synapse formation to ensure appropriate neural connectivity in the physiological state. However, increased C1q expression in pathological states may induce microglia to over-phagocytose synapses, ultimately leading to CNS disease [44]. It has been reported that C1q expression is increased in the hippocampus and prefrontal cortex of a mouse model of Alzheimer's disease, and that the inhibition of C1q expression or the antagonism of its receptor can reduce phagocytic microglial numbers and synaptic loss [30]. Moreover, aged C1q-deficient mice exhibit enhanced synaptic plasticity and hippocampus-dependent memory [45]. Consistent with these previous reports, our results indicate that increased C1q leads to excessive synaptic phagocytosis by microglia in the hippocampal CA1 region of SAE model mice, and that this can be inhibited by CCK8 injection. Furthermore, our previous study indicated that CCK8 intraperitoneal injection decreases C1q expression by inhibiting microglial activation in mice with delayed neurocognitive recovery [8], which provides additional support to the results of the present study. Taken together, our findings suggest that microglia-induced activation of the complement system is a common pathogenic mechanism of both delayed neurocognitive recovery and SAE. Moreover, C1q can induce the polarisation of neurotoxic A1 astrocytes and indirectly affect the structure and function of synapses [15], and we noted that A1 astrocyte numbers were significantly increased in the CA1 region of SAE model mice, whereas CCK8 suppressed this increase. We thus speculate that the CCK8-induced inhibition of C1q expression may subsequently affect excitatory synaptic plasticity in the hippocampal CA1 region of SAE model mice through two pathways: first, by inhibiting the microglial phagocytosis of synapses, and second, by supressing the synaptic toxicity induced by A1 astrocytes.

There were several limitations in the present study. First, we only used murine BV2 microglial cells for the in vitro experiments. It therefore remains to be further investigated whether the results of our experiments can be replicated in primary mouse or human microglia. Second, 5 mg/kg LPS caused short-term cognitive impairments in SAE model mice in the present study. By contrast, cecum ligation and puncture or higher doses of LPS result in relatively long-term cognitive impairments. Thus, it remains unclear whether CCK8 and dorsal hippocampal CCK-positive neurons play a role in alleviating more severe cognitive impairments in SAE model mice; this warrants further investigation. Third, synaptic plasticity is the cellular and morphological basis of learning and memory [46]. Although our study suggests that CCK8 can reverse the damage to synaptic plasticity and cognitive function in SAE mice, it cannot be ruled out

that CCK8 may affect cognitive function through other pathways.

Conclusions

The findings from the present study indicate that CCK inhibits C1q expression through microglial CCK2R, thus attenuating C1q-mediated synaptic plasticity damage and ultimately improving cognitive dysfunction in SAE model mice. Both CCK drugs and specific activation of CCK-positive neurons are potential treatments for SAE.

Abbreviations

ACSF	Artificial cerebrospinal fluid
CA1	Cornu ammonis 1
CCK	Cholecystokinin
CNS	Central nervous system
C1q	Complement 1q
DG	Dentate gyrus
ELISA	Enzyme-linked immunosorbent assay
FCT	Fear conditioning test
LPS	Lipopolysaccharide
mEPSCs	Miniature excitatory postsynaptic currents
MWM	Morris water maze
PBS	Phosphate-buffered saline
qPCR	Quantitative real-time polymerase chain reaction
SAE	Sepsis-associated encephalopathy
SD	Standard deviation
sEPSCs	Spontaneous excitatory postsynaptic currents

Supplementary Information

The online version contains supplementary material available at https://doi.org/10.1186/s12974-025-03554-9.

Supplementary Material 1.

Acknowledgements

We thank Miao He, PhD, for providing the CCK-Cre mice, and Bronwen Gardner, PhD, from Liwen Bianji (Edanz) (www.liwenbianji.cn/) for editing the English text of a draft of this manuscript.

Authors' contributions

LC, TTL, ZQL, and XYG designed the experiment. LC, ZL, YBG and GXP performed the experiment. LC, ZL, JW and ZQL collected and analyzed the data and prepared the manuscript. LC, ALD, YTL and JSH were involved in preparing the animal models and participated in interpreting the results. LC and QW contributed to behavioral testing. LC and KXL were involved in biochemical analysis. LC and Z L participated in the statistical analysis. LC, LHC, TTL, ZQL and XYG contributed to the study concept and design, secured funding for the project, and prepared and critically revised the manuscript. All authors reviewed the manuscript.

Funding

This study was supported by the National Natural Science Foundation of China (82401505, 82101265, 82271222), China Postdoctoral Science Foundation (2023M740142), China Postdoctoral Fellowship Program (GZC20230143) and Research Project of Peking University Third Hospital in State Key Laboratory of Vascular Homeostasis and Remodeling (Peking University) (2024-VHR-SY-10).

Data availability

No datasets were generated or analysed during the current study.

Declarations

Ethics approval and consent to participate

All animal care and experimental procedures were approved by the animal ethics committee of Peking University Health Science Center (ethics number: LA2021534).

Consent for publication

Not applicable.

Competing interests

The authors declare no competing interests.

Author details

[1]Department of Anesthesiology, Peking University Third Hospital, Beijing 100191, China
[2]Department of Anesthesiology and Pain Medicine, Tongji Hospital of Tongji Medical College, Huazhong University of Science and Technology, Wuhan 430030, Hubei, China
[3]Department of Anesthesiology and Perioperative Medicine, General Hospital of Ningxia Medical University, Yinchuan, Ningxia 750004, China
[4]Department of Anesthesiology, Jilin Provincial People's Hospital, Changchun, Jilin 130022, China
[5]Department of Neurology, Shanghai Key Laboratory of Emotions and Affective Disorders, Songjiang Research Institute, Songjiang Hospital, Shanghai Jiao Tong University School of Medicine, Shanghai 201600, China
[6]Institute of Neuroscience and Brain Diseases, Xiangyang Central Hospital, Affiliated Hospital of Hubei University of Arts and Science, Xiangyang 441000, Hubei, China
[7]Department of Rehabilitation Sciences, Faculty of Health and Social Sciences, The Hong Kong Polytechnic University, Hong Kong 999077, China
[8]Research Institute for Smart Ageing (RISA), The Hong Kong Polytechnic University, Hong Kong 999077, China
[9]Mental Health Research Center (MHRC), The Hong Kong Polytechnic University, Hong Kong 999077, China
[10]State Key Laboratory of Vascular Homeostasis and Remodeling, Peking University Third Hospital, Beijing 100191, China
[11]State Key Laboratory of Vascular Homeostasis and Remodeling, Department of Anesthesiology, Peking University Third Hospital, Beijing 100191, China

Received: 14 January 2025 / Accepted: 3 September 2025
Published online: 29 September 2025

References

1. Gofton TE, Young GB. Sepsis-associated encephalopathy. Nat Rev Neurol. 2012;8(10):557–66.
2. Golzari SE, Mahmoodpoor A. Sepsis-associated encephalopathy versus sepsis-induced encephalopathy. Lancet Neurol. 2014;13(10):967–8.
3. Nwafor DC, Brichacek AL, Mohammad AS, Griffith J, Lucke-Wold BP, Benkovic SA, et al. Targeting the blood-brain barrier to prevent Sepsis-Associated cognitive impairment. J Cent Nerv Syst Dis. 2019;11:1179573519840652.
4. Luo RY, Luo C, Zhong F, Shen WY, Li H, Hu ZL, et al. ProBDNF promotes sepsis-associated encephalopathy in mice by dampening the immune activity of meningeal CD4(+) T cells. J Neuroinflammation. 2020;17(1):169.
5. Catarina AV, Branchini G, Bettoni L, De Oliveira JR, Nunes FB. Sepsis-associated encephalopathy: from pathophysiology to progress in experimental studies. Mol Neurobiol. 2021;58(6):2770–9.
6. Hallberg M. Neuropeptides: metabolism to bioactive fragments and the pharmacology of their receptors. Med Res Rev. 2015;35(3):464–519.
7. Plagman A, Hoscheidt S, McLimans KE, Klinedinst B, Pappas C, Anantharam V, et al. Cholecystokinin and Alzheimer's disease: a biomarker of metabolic function, neural integrity, and cognitive performance. Neurobiol Aging. 2019;76:201–7.
8. Chen L, Yang N, Li Y, Li Y, Hong J, Wang Q, et al. Cholecystokinin octapeptide improves hippocampal glutamatergic synaptogenesis and postoperative cognition by inhibiting induction of A1 reactive astrocytes in aged mice. CNS Neurosci Ther. 2021;27(11):1374–84.

9. Voits M, Hasenöhrl RU, Huston JP, Fink H. Repeated treatment with cholecystokinin octapeptide improves maze performance in aged Fischer 344 rats. Peptides. 2001;22(8):1325–30.
10. Lau SH, Young CH, Zheng Y, Chen X. The potential role of the cholecystokinin system in declarative memory. Neurochem Int. 2023;162:105440.
11. Chen L, Dong R, Lu YY, Zhou Y, Li K, Zhang ZZ, et al. Microrna-146a protects against cognitive decline induced by surgical trauma by suppressing hippocampal neuroinflammation in mice. Brain Behav Immun. 2019;78:188–201.
12. Wang C, Yue H, Hu Z, Shen Y, Ma J, Li J, et al. Microglia mediate forgetting via complement-dependent synaptic elimination. Science. 2020;367(6478):688–94.
13. Schafer DP, Lehrman EK, Kautzman AG, Koyama R, Mardinly AR, Yamasaki R, et al. Microglia sculpt postnatal neural circuits in an activity and complement-dependent manner. Neuron. 2012;74(4):691–705.
14. Dejanovic B, Huntley MA, De Mazière A, Meilandt WJ, Wu T, Srinivasan K, et al. Changes in the synaptic proteome in tauopathy and rescue of Tau-Induced synapse loss by C1q antibodies. Neuron. 2018;100(6):1322–e13367.
15. Liddelow SA, Guttenplan KA, Clarke LE, Bennett FC, Bohlen CJ, Schirmer L, et al. Neurotoxic reactive astrocytes are induced by activated microglia. Nature. 2017;541(7638):481–7.
16. Gou H, Sun D, Hao L, An M, Xie B, Cong B, et al. Cholecystokinin-8 attenuates methamphetamine-induced inflammatory activation of microglial cells through CCK2 receptor. Neurotoxicology. 2020;81:70–9.
17. Percie du Sert N, Hurst V, Ahluwalia A, Alam S, Avey MT, Baker M, et al. The ARRIVE guidelines 2.0: updated guidelines for reporting animal research. J Cereb Blood Flow Metab. 2020;40(9):1769–77.
18. Ge C, Chen W, Zhang L, Ai Y, Zou Y, Peng Q. Chemogenetic activation of the HPC-mPFC pathway improves cognitive dysfunction in lipopolysaccharide -induced brain injury. Theranostics. 2023;13(9):2946–61.
19. Shrum B, Anantha RV, Xu SX, Donnelly M, Haeryfar SM, McCormick JK, et al. A robust scoring system to evaluate sepsis severity in an animal model. BMC Res Notes. 2014;7:233.
20. Anderson ST, Commins S, Moynagh PN, Coogan AN. Lipopolysaccharide-induced sepsis induces long-lasting affective changes in the mouse. Brain Behav Immun. 2015;43:98–109.
21. Zhang W, Huang J, Gao F, You Q, Ding L, Gong J, et al. *Lactobacillus reuteri* normalizes altered fear memory in male Cntnap4 knockout mice. EBioMedicine. 2022;86:104323.
22. Chu X, Cao L, Yu Z, Xin D, Li T, Ma W, et al. Hydrogen-rich saline promotes microglia M2 polarization and complement-mediated synapse loss to restore behavioral deficits following hypoxia-ischemic in neonatal mice via AMPK activation. J Neuroinflammation. 2019;16(1):104.
23. Nguyen SMT, Rupprecht CP, Haque A, Pattanaik D, Yusin J, Krishnaswamy G. Mechanisms governing anaphylaxis: inflammatory cells, mediators, endothelial gap junctions and beyond. Int J Mol Sci. 2021. https://doi.org/10.3390/ijms22157785.
24. Li Z, Yin P, Chen J, Li C, Liu J, Rambojan H, et al. Activation of the extracellular signal-regulated kinase in the amygdale modulates Fentanyl-induced hypersensitivity in rats. J Pain. 2017;18(2):188–99.
25. Li Z, Sun T, He Z, Li Z, Zhang W, Wang J, et al. Scfas ameliorate chronic post-surgical pain-related cognition dysfunction via the ACSS2-HDAC2 axis in rats. Mol Neurobiol. 2022;59(10):6211–27.
26. Chen L, Li S, Zhou Y, Liu T, Cai A, Zhang Z, et al. Neuronal mechanisms of adenosine A(2A) receptors in the loss of consciousness induced by Propofol general anesthesia with functional magnetic resonance imaging. J Neurochem. 2021;156(6):1020–32.
27. Vizcaychipi MP, Xu L, Barreto GE, Ma D, Maze M, Giffard RG. Heat shock protein 72 overexpression prevents early postoperative memory decline after orthopedic surgery under general anesthesia in mice. Anesthesiology. 2011;114(4):891–900.
28. Vorhees CV, Williams MT. Morris water maze: procedures for assessing spatial and related forms of learning and memory. Nat Protoc. 2006;1(2):848–58.
29. Chen X, Li X, Wong YT, Zheng X, Wang H, Peng Y, et al. Cholecystokinin release triggered by NMDA receptors produces LTP and sound-sound associative memory. Proc Natl Acad Sci U S A. 2019;116(13):6397–406.
30. Hong S, Beja-Glasser VF, Nfonoyim BM, Frouin A, Li S, Ramakrishnan S, et al. Complement and microglia mediate early synapse loss in Alzheimer mouse models. Science. 2016;352(6286):712–6.
31. Schartz ND, Tenner AJ. The good, the bad, and the opportunities of the complement system in neurodegenerative disease. J Neuroinflammation. 2020;17(1):354.
32. Wang X, Li X, Zuo X, Liang Z, Ding T, Li K, et al. Photobiomodulation inhibits the activation of neurotoxic microglia and astrocytes by inhibiting Lcn2/JAK2-STAT3 crosstalk after spinal cord injury in male rats. J Neuroinflammation. 2021;18(1):256.
33. Asrican B, Wooten J, Li YD, Quintanilla L, Zhang F, Wander C, et al. Neuropeptides modulate local astrocytes to regulate adult hippocampal neural stem cells. Neuron. 2020;108(2):349–e3666.
34. Petrella C, Di Certo MG, Barbato C, Gabanella F, Ralli M, Greco A, et al. Neuropeptides in Alzheimer's disease: an update. Curr Alzheimer Res. 2019;16(6):544–58.
35. Shen YC, Sun X, Li L, Zhang HY, Huang ZL, Wang YQ. Roles of neuropeptides in sleep-wake regulation. Int J Mol Sci. 2022. https://doi.org/10.3390/ijms23094599.
36. Borbély E, Scheich B, Helyes Z. Neuropeptides in learning and memory. Neuropeptides. 2013;47(6):439–50.
37. Neugebauer V, Mazzitelli M, Cragg B, Ji G, Navratilova E, Porreca F. Amygdala, neuropeptides, and chronic pain-related affective behaviors. Neuropharmacology. 2020;170:108052.
38. Holzer P, Farzi A. Neuropeptides and the microbiota-gut-brain axis. Adv Exp Med Biol. 2014;817:195–219.
39. Liu YJ, Liu TT, Jiang LH, Liu Q, Ma ZL, Xia TJ, et al. Identification of hub genes associated with cognition in the hippocampus of Alzheimer's disease. Bioengineered. 2021;12(2):9598–609.
40. Xiong B, Zhang W, Zhang L, Huang X, Zhou W, Zou Q, et al. Hippocampal glutamatergic synapses impairment mediated novel-object recognition dysfunction in rats with neuropathic pain. Pain. 2020;161(8):1824–36.
41. Yin XY, Tang XH, Wang SX, Zhao YC, Jia M, Yang JJ, et al. Hmgb1 mediates synaptic loss and cognitive impairment in an animal model of sepsis-associated encephalopathy. J Neuroinflammation. 2023;20(1):69.
42. Dehghani F, Reisi P. Acute application of cholecystokinin and its effect on long-term potentiation induction at CA1 area of hippocampal formation in rat. Physiol Pharmacol. 2015;19:241–6.
43. Fouët G, Bally I. Molecular basis of complement C1q collagen-like region interaction with the immunoglobulin-like receptor LAIR-1. Int J Mol Sci. 2021. https://doi.org/10.3390/ijms22105125.
44. Cornell J, Salinas S, Huang HY, Zhou M. Microglia regulation of synaptic plasticity and learning and memory. Neural Regen Res. 2022;17(4):705–16.
45. Stephan AH, Madison DV, Mateos JM, Fraser DA, Lovelett EA, Coutellier L, et al. A dramatic increase of C1q protein in the CNS during normal aging. J Neurosci. 2013;33(33):13460–74.
46. Ohm M, Hosseini S, Lonnemann N, He W, More T, Goldmann O, et al. The potential therapeutic role of itaconate and mesaconate on the detrimental effects of LPS-induced neuroinflammation in the brain. J Neuroinflammation. 2024;21(1):207.

Publisher's Note